



Article

Tribological Performance of CF-PEEK Sliding against 17-4PH Stainless Steel with Various Cermet Coatings for Water Hydraulic Piston Pump Application

Songlin Nie , Fangli Lou, Hui Ji *  and Fanglong Yin

Beijing Key Laboratory of Advanced Manufacturing Technology, Beijing University of Technology,
Beijing 100124, China

* Correspondence: jihui@bjut.edu.cn; Tel.: +86-10-6739-6362; Fax: +86-10-6739-1617

Received: 19 June 2019; Accepted: 5 July 2019; Published: 11 July 2019



Abstract: To improve the abrasion resistance performance of the critical tribopairs within water hydraulic piston pumps, tribological characteristics of the stainless steel 17-4PH and 17-4PH coated with $\text{Cr}_3\text{C}_2\text{-NiCr}$, WC-10Co-4Cr , Cr_2O_3 and $\text{Al}_2\text{O}_3\text{-13\%TiO}_2$ sliding against carbon fiber reinforced polyetheretherketone (CF-PEEK) composite under water-lubricated condition were experimentally studied using a pin-on-ring test bench with different working conditions. It has been demonstrated by the experimental results that the tribological behaviors of CF-PEEK/cermet coatings tribopairs were better than that of CF-PEEK/17-4PH tribopair under water lubrication. However, the $\text{Cr}_3\text{C}_2\text{-NiCr}$ coating could be damaged under high rotational speed. Due to the reaction film produced by the $\text{Al}_2\text{O}_3\text{-13\%TiO}_2$ and water, the CF-PEEK/ $\text{Al}_2\text{O}_3\text{-13\%TiO}_2$ material combination exhibits more excellent tribological behaviors than other tribopairs lubricated with water, and could preferentially be used in water hydraulic piston pumps.

Keywords: tribological performance; cermet coating; CF-PEEK; water lubrication

1. Introduction

Water hydraulic power transmission has been widely used in the food processing industry, chemical and pharmaceutical industry, water mist fire extinguishing and seawater reverse osmosis desalination system due to its environmental friendliness, cleanliness of working media, low operation cost and high efficiency [1–5]. Figure 1 illustrates the structure of a water hydraulic axial piston pump (WHAPP), which is a critical power component of water hydraulic transmission system. It should be noted that all of the tribopairs in WHAPP are directly lubricated with water. Therefore, there are some challenging problems in the development of high-reliability WHAPPs. For example, the bad lubrication, strong corrosiveness and low viscosity of water could lead to early failure of the critical tribopairs (such as the slipper/swash-plate, sliding bearing/cylinder, piston/cylinder, valve-plate/port-plate tribopairs) in WHAPP (as shown in Figure 1) [6]. Consequently, the use of materials of the critical tribopairs in WHAPP with low friction and resistant to wear underwater lubrication condition is important.

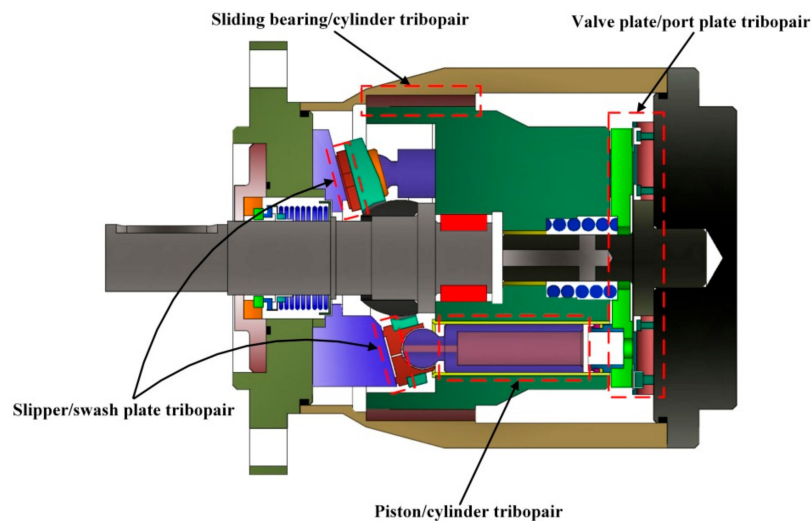


Figure 1. Configurations of a water hydraulic axial piston pump.

The tribopairs consisting of stainless steel and reinforced polymer PEEK have been applied successfully in the water hydraulic components with medium-high pressure (working pressure less than 16 MPa) [7]. However, when using this material combination, the working water medium should be filtered through a high precision filter with 10 μm absolute filtering accuracy. This is due to the fact that the stainless steel is not the best material for water hydraulic pumps to overcome friction and wear because of its relatively low hardness (lower than HRC 50) [8]. Fortunately, several reports have demonstrated that cermet and ceramic coatings have excellent tribological characteristics especially lubricated with air, oil and water [9–11]. Huang et al. [12] researched the friction and wear properties of Ti (C, N) cermet coupled with Si_3N_4 engineering ceramic lubricated with water. It is demonstrated that super-low friction coefficient can be detected with a 2 N applied load. Wu et al. [13] studied the tribological performance of WC-10Co-4Cr coating sliding against Si_3N_4 lubricated with silt-laden water. It was concluded that the deposition of SiO_2 and $\text{Si}(\text{OH})_4$ layers produced by the tribo-chemical reaction between water and Si_3N_4 can significantly reduce the friction and wear of the friction pair. In other research [14], they investigated the tribological characteristics of different mass ratio Al_2O_3 -13% TiO_2 coatings coupled with Si_3N_4 lubricated with water. It has been demonstrated that the material combination of Al_2O_3 -13% TiO_2 / Si_3N_4 is an appropriate scheme to use in water hydraulic components. Wang et al. [15] studied the friction and characteristics of Cr/graphite-like carbon (GLC) coating coupled with Al_2O_3 , ZrO_2 , SiC, Si_3N_4 and WC under seawater lubrication condition. It was found that the combination of Cr/GLC coating and Si_3N_4 ceramic presented the optimum tribological performance. Strmčnik et al. [16] presented an investigation on the tribological behaviors of AISI 440C ball coupled with diamond-like carbon (DLC) coated disk under water lubrication condition for orbital hydraulic motor application. It was concluded that the wear coefficient for the DLC coating was about $10^{-9} \text{ mm}^3/\text{Nm}$, and the friction coefficient of this tribopair in water was lower than that under oil lubrication conditions. Qiu et al. [17] comparatively researched the wear properties of different material combinations of 316L, surface treatment 316L, and PEEK with 30% carbon fiber in water. It has been demonstrated that the combination of 316L with surface treatment of tetrahedral amorphous carbon and PEEK with 30% carbon fiber presented the optimum friction characteristics. Zhu et al. [18] concluded that the tribological performance of $\text{Ni}_3\text{Al-Ag}/\text{Al}_2\text{O}_3$ tribopair is better than that of SiC/316L tribopair in a seawater environment. Therefore, coating the stainless steel with cermet and engineering ceramic may be an effective way to improve the abrasion resistance performance of the tribopairs in WHAPP. In addition, carbon fiber reinforced polyetheretherketone (CF-PEEK) has excellent wear-resistance and tribological behaviors in water. And the friction and wear properties of CF-PEEK coupled with 17-4PH stainless steel have been comprehensively investigated [19–22]. The experimental results indicated that

the tribological performance of CF-PEEK mating with 17-4PH stainless steel in seawater is excellent, which can be used in high-pressure seawater hydraulic components.

Though several papers are available on tribology of cermet/engineering ceramic and PEEK/stainless steel tribopairs in water, adequate data are not available on the tribological performance of CF-PEEK coupled with different cermet coatings for WHAPP application. Therefore, in this paper, several kinds of cermet coatings have been manufactured by using high-velocity oxygen-fuel (HVOF) technology. A comparative study on the friction and wear properties of the CF-PEEK coupled with 17-4PH stainless steel, $\text{Cr}_3\text{C}_2\text{-NiCr}$, WC-10Co-4Cr , Cr_2O_3 and $\text{Al}_2\text{O}_3\text{-13\%TiO}_2$ coatings will be conducted underwater lubrication condition.

2. Experiments

2.1. Specimens Introduction

The upper pin was made of CF-PEEK and contained 30% volume fraction of carbon fiber, polytetrafluoroethylene and graphite formed through hot-pressing, sintering and molding technology [22]. The physical properties of CF-PEEK composite are shown in Table 1. The lower disk was made of 17-4PH stainless steel, and the surface hardness of the lower specimens was improved by solution and aging treatment before being sprayed (the hardness of 17-4PH is about HRC 45). Then, several cermet coatings were sprayed on the surface of 17-4PH stainless steel using the HVOF technique respectively. Table 2 lists the main chemical contents of 17-4PH stainless steel. In addition, the major physical performance parameters of the cermet coatings are shown in Table 3. Before each tribological test, the contacting surface roughness of the CF-PEEK and cermet coatings specimens was approximately $0.1\text{ }\mu\text{m}$ by grinding, diamond anti-scuffing paste polishing and metallographic sandpaper. Furthermore, all the upper pins and lower disks were immersed in water for more than 168 h to remove the influence of water absorption on the weight of the specimens during the tribological test.

Table 1. Main physical properties of carbon fiber reinforced polyetheretherketone (CF-PEEK) composite.

Property	Standard	Unit	Value
Density	ISO 1183	g/cm^3	1.44
Water Absorption (24 h, 23 °C)	ISO 62	%	0.06
Rockwell Hardness	ASTM D785	—	102
Tensile Strength (23 °C)	ASTM D638	MPa	134
Bending Strength (23 °C)	ASTM D790	MPa	186
Compressive Strength (23 °C)	ASTM D695	MPa	150
Coefficient of Thermal Expansion	ASTM D696	$10^{-5}/^\circ\text{C}$	2.2

Table 2. Main chemical contents of 17-4PH stainless steel (wt.%).

C	Si	Mn	P	Cr	Ni
≤ 0.07	≤ 1.00	≤ 1.00	≤ 0.035	15.5–17.5	3.0–5.0

Table 3. Main physical performance of $\text{Cr}_3\text{C}_2\text{-NiCr}$, WC-10Co-4Cr , Cr_2O_3 and $\text{Al}_2\text{O}_3\text{-13\%TiO}_2$ coatings.

Property	$\text{Cr}_3\text{C}_2\text{-NiCr}$	WC-10Co-4Cr	Cr_2O_3	$\text{Al}_2\text{O}_3\text{-13\%TiO}_2$
Density (g/cm^3)	5.92	5.40	5.21	3.6
Vickers Hardness (HV 0.3)	890	1300	1620	840
Elasticity Modulus (GPa)	60	150	75	170
Bending Strength (MPa)	126	113	132	23.5

2.2. Test Rig and Methods

The tribological tests were performed in a rotational friction tester (UMT TriboLab, Bruker, Billerica, MA, USA) using pin-on-disk mode (as shown in Figure 2). The UMT TriboLab (version 1.143) applied a programmable load downward by a servo-driven carriage. In addition the two-dimensional force sensor (Bruker, Billerica, MA, USA) (up to 200 N load) was used to detect the sliding and frictional force between the material combination. During the tests, the lower disk was rotational whereas the upper pin was always stationary. Moreover, a specially designed recirculating liquid holder was provided for testing surfaces immersed in water. The fluid recirculated naturally as the motion of the test surface forced the fluid through apertures in a specially designed chamber and then back to the top of the specimens.

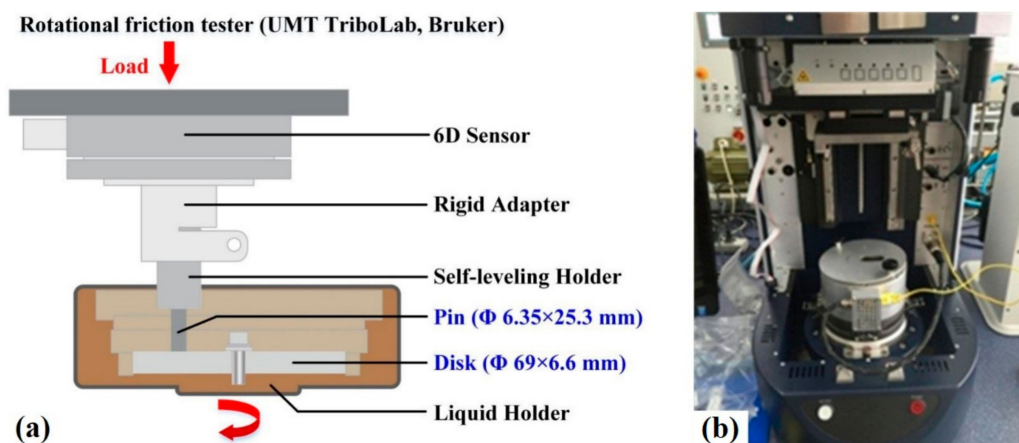


Figure 2. Schematic configuration of the pin-on-disk test: (a) schematic diagram; (b) real photo.

The tests were conducted at a load of 100 N, rotational speeds of 100 and 300 r/min, ambient temperature, and the time for each tribological test was 60 min. Due to the limitation of the test operating condition, the experimental parameters of this research were lower than the real working load and velocity of the tribopairs in WHAPP under the operating pressure of 14 MPa. However, the pin-to-disk contacting model was similar to the slipper/swash-plate and valve-plate/port-plate tribopairs, and the tribological tests can also compare the advantages and disadvantages of the proposed material combinations, providing a basis for the material matching of WHAPP. Before and after each test, all the specimens were ultrasoniclly cleaned in anhydrous alcohol and dried with hot air. Then, the weight loss Δm can be obtained by the electronic balance (Ohaus CP214, Parsippany, NJ, USA) with an accuracy of 0.1 mg. The wear rate W_s can be obtained as follows:

$$W_s = \frac{\Delta m}{\rho F_N L} \left(\text{mm}^3 / \text{Nm} \right) \quad (1)$$

where ρ represents the density of the specimens, F_N is the applied load, L is the total sliding distance. During the tribological test, the software of UMT TriboLab can collect the dynamic friction coefficient of the tribopairs and other data in real-time. Each test was repeated at least three times for eliminating occasionality of the experimental results under the same working conditions.

To reveal the friction and wear mechanism of the tribopairs, the surface morphology of the CF-PEEK pin and the coupled disk were analyzed by a scanning electron microscope (SEM, SU3500, Hitachi, Tokyo, Japan) equipped with energy dispersive spectroscopy (EDS, EDAX, Berwyn, IL, USA). And a digital microscope (VHX-5000, Keyence, Osaka, Japan) was employed to examine the 3D topographies of the wear track.

3. Results and Discussion

3.1. Friction and Wear Behavior

Friction coefficients of CF-PEEK composite coupled with several cermet coatings in water under 100 N load and 100 r/min, 300 r/min rotational speeds are shown in Figure 3. It is illustrated in Figure 3 that the friction coefficient of each tribopair increased firstly, then decreased slightly, and finally achieved a stable value after experiencing the running-in process. When sliding at 100 r/min, the CF-PEEK/WC-10Co-4Cr tribopair did not operate steadily. Nevertheless, the friction coefficients of other tribopairs were rapidly stable after a short running-in process under both 100 and 300 r/min. By comparing Figure 3a,b, it was observed that the friction coefficients of all the tribopairs decreased when the rotational speed increased from 100 to 300 r/min. It can be seen from Figure 3c that the mean friction coefficients of the tested five material combinations with two rotational speeds are below 0.2. As sliding under 100 r/min rotational speed, the friction coefficient of Cr_2O_3 was almost equal to 0.17, which was higher than those of other tribopairs. As the rotational speed increased to 300 r/min, the mean friction coefficients of 17-4PH stainless steel, $\text{Cr}_3\text{C}_2\text{-NiCr}$, WC-10Co-4Cr, Cr_2O_3 and $\text{Al}_2\text{O}_3\text{-13TiO}_2$ coatings reduced to 0.133, 0.155, 0.135 and 0.097 respectively. The above experimental results clearly demonstrate that the friction coefficient of $\text{Al}_2\text{O}_3\text{-13TiO}_2$ was lower than those of other tribopairs under high rotational speed.

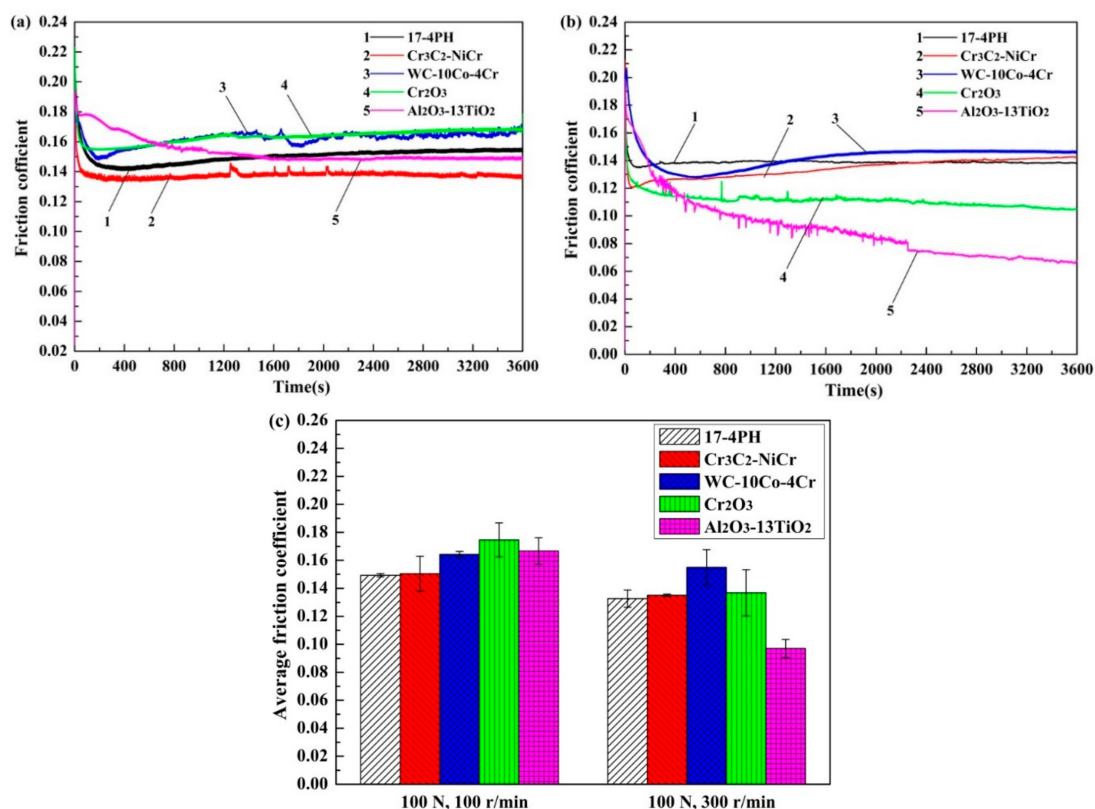


Figure 3. Friction coefficients of 17-4PH and several coatings sliding against CF-PEEK: (a) 100 N, 100 r/min; (b) 100 N, 300 r/min and (c) the mean friction coefficients.

The wear rates of the CF-PEEK composite, 17-4PH stainless steel and cermet coatings are shown in Figure 4. It should be noted from Figure 4a that the wear rates of CF-PEEK/cermet coatings tribopairs were lower than that of CF-PEEK/17-4PH tribopair. As clearly presented in Figure 4a, the wear rate of CF-PEEK was lowest when sliding against $\text{Al}_2\text{O}_3\text{-13TiO}_2$ coating. When the rotational speed increased from 100 to 300 r/min, the wear rate of CF-PEEK composites had a similar trend with that of the friction coefficient. Additionally, it is clearly illustrated in Figure 4a,b that the wear rates of

CF-PEEK composites were much higher than those of 17-4PH stainless steel. Furthermore, the cermet coatings exhibited negative wear rates under 100 N and 300 r/min, so it is inferred that some CF-PEEK composites were transferred to the coating surface. However, the wear rate of $\text{Cr}_3\text{C}_2\text{-NiCr}$ coating was higher than those of 17-4PH and other cermet coatings, which may be attributed to the damage and spalling of the $\text{Cr}_3\text{C}_2\text{-NiCr}$ coating under high rotational speed.

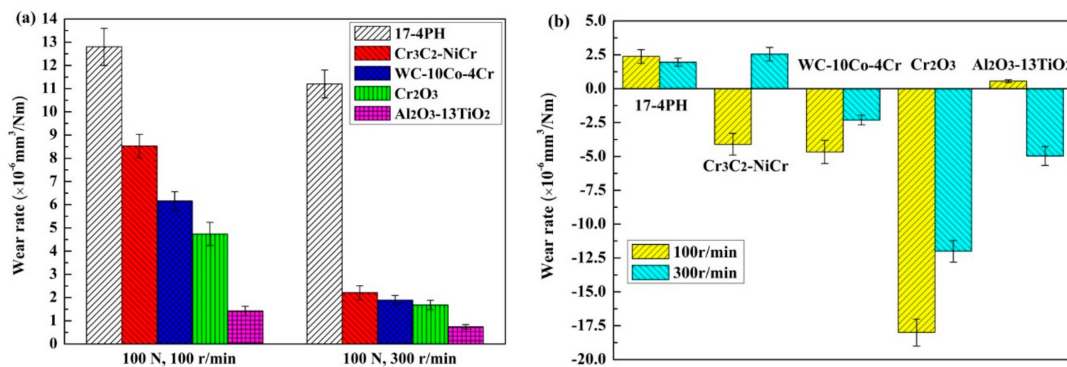


Figure 4. The wear rates of several tribopairs: (a) wear rates of CF-PEEK polymers and (b) wear rates of 17-4PH and several cermet coatings.

As a result, it can be concluded that the 17-4PH and cermet coatings presented better friction and wear behavior under a rotational speed of 300 r/min than 100 r/min. Moreover, the CF-PEEK/ $\text{Al}_2\text{O}_3\text{-13}\%\text{TiO}_2$ coating tribopair exhibited better tribological performance in terms of wear than other tribopairs lubricated with water.

3.2. Analyses of the Worn Surfaces Lubricated with Water

Figure 5 shows SEM images of CF-PEEK composites against 17-4PH stainless steel and four kinds of cermet coatings at the 100 N applied load and 300 r/min rotational speed lubricated with water. It can easily be seen that the worn surface of CF-PEEK/ $\text{Al}_2\text{O}_3\text{-13}\%\text{TiO}_2$ tribopair is smoothest, and only a spot of CF-PEEK debris can be observed (Figure 5e). As illustrated in Figure 5a,b, some carbon fibers were exposed to the contacting surface as a result of abrasive wear and slight adhesion wear. When sliding against WC-10Co-4Cr, it can be seen from Figure 5c that the CF-PEEK contacting surface was characterized by severe plastic deformation and partly broken due to the grinding process. As shown in Figure 5d, CF-PEEK exhibited serious adhesion wear for the Cr_2O_3 coating, and large patches of deformed layers (caused by softened matrix material) covered the worn surface, which caused some CF-PEEK composites to tear apart. This is related to the relatively high surface hardness of Cr_2O_3 coating (about 1620 Hv) compared to those of 17-4PH and other cermet coatings, which could lead to the severe wear of the soft CF-PEEK composite. Therefore, it can be concluded that the large hardness difference between the CF-PEEK and cermet coatings could accelerate the wear of the soft CF-PEEK.

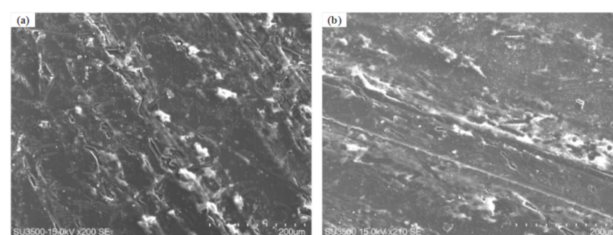


Figure 5. Cont.

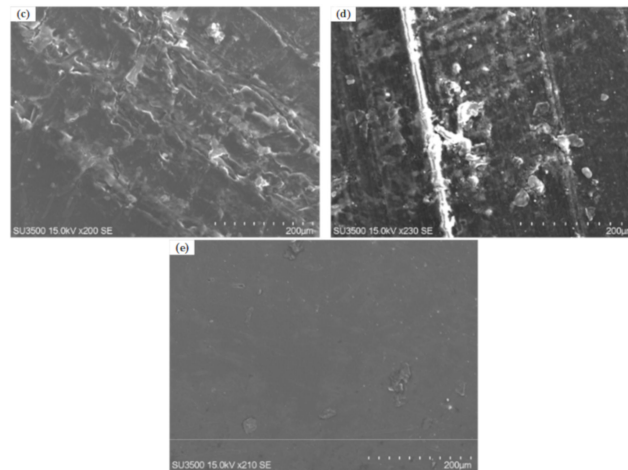


Figure 5. Worn surfaces morphology of CF-PEEK when sliding against 17-4PH and several cermet coatings (100 N, 300 r/min): (a) CF-PEEK/17-4PH; (b) CF-PEEK/Cr₃C₂-NiCr; (c) CF-PEEK/WC-10Co-4Cr; (d) CF-PEEK/Cr₂O₃ and (e) CF-PEEK/Al₂O₃-13%TiO₂.

Figure 6 demonstrates the worn surface morphology and EDS data of 17-4PH stainless steel, Cr₃C₂-NiCr, WC-10Co-4Cr, Cr₂O₃ and Al₂O₃-13%TiO₂ coatings under 100 N and 300 r/min. It is evident from Figure 6a–c that some wear scratches existed on the contacting surfaces owing to the sliding friction along the circumferential direction. As illustrated in Figure 6a, the 17-4PH worn surface mainly contained abrasion marks characterized as deep furrows produced by ploughing processes, and some black wear debris was embedded in the wear track. The corresponding EDS analysis of 17-4PH surface displayed that the wear debris mainly contained Fe, Cr and C elements. Moreover, the detected content of C element from Figure 6a was more than that of original 17-4PH stainless steel (as listed in Table 2). This indicates that some elements transferred from the CF-PEEK surface to the 17-4PH surface during the tribological test. In Figure 6b, some wear debris and shallow furrows appeared on the surface of Cr₃C₂-NiCr coating. In addition, it should be noted in Figure 6b that the surface of Cr₃C₂-NiCr coating was slightly rough and characterized with some spalling pits, suggesting the damage and spalling of the Cr₃C₂-NiCr coating under 100 N and 300 r/min. Besides, the detected content of C element also demonstrated the transfer of CF-PEEK to the surface of the Cr₃C₂-NiCr coating. As illustrated in Figure 6c, some tiny scratches and wear debris can be found on the pretty smooth worn surface of WC-10Co-4Cr. However, it can be seen from Figure 6d,e that the wear surfaces of Cr₂O₃ and Al₂O₃ coatings were characterized by the micropores instead of wear furrows, and no indication of adhesive wear was found. It is inferred the water inside the micropores was instrumental in improving the lubrication and heat dissipation conditions. In the comparison of Figure 6d,e, one disparity was noticeable that more micropores and sporadic wear debris appeared on Cr₂O₃ coating worn surface, which is consistent with the results of negative wear rates of Cr₂O₃ coating in Figure 4. In addition, this indicated that more Cr₂O₃ coating and CF-PEEK particles pell off during the sliding process, and then the contacting surface roughness would be increased as well as the friction coefficient of this material combination. Moreover, it is interesting to note from Figure 6 that the content of C element on Al₂O₃-13%TiO₂ surface was the smallest among those of the lower specimens. This indicates that the minimum wear-loss and transfer of CF-PEEK could be obtained when sliding against Al₂O₃-13%TiO₂ coating, which is in agreement with the results of wear rates in Figure 4a.

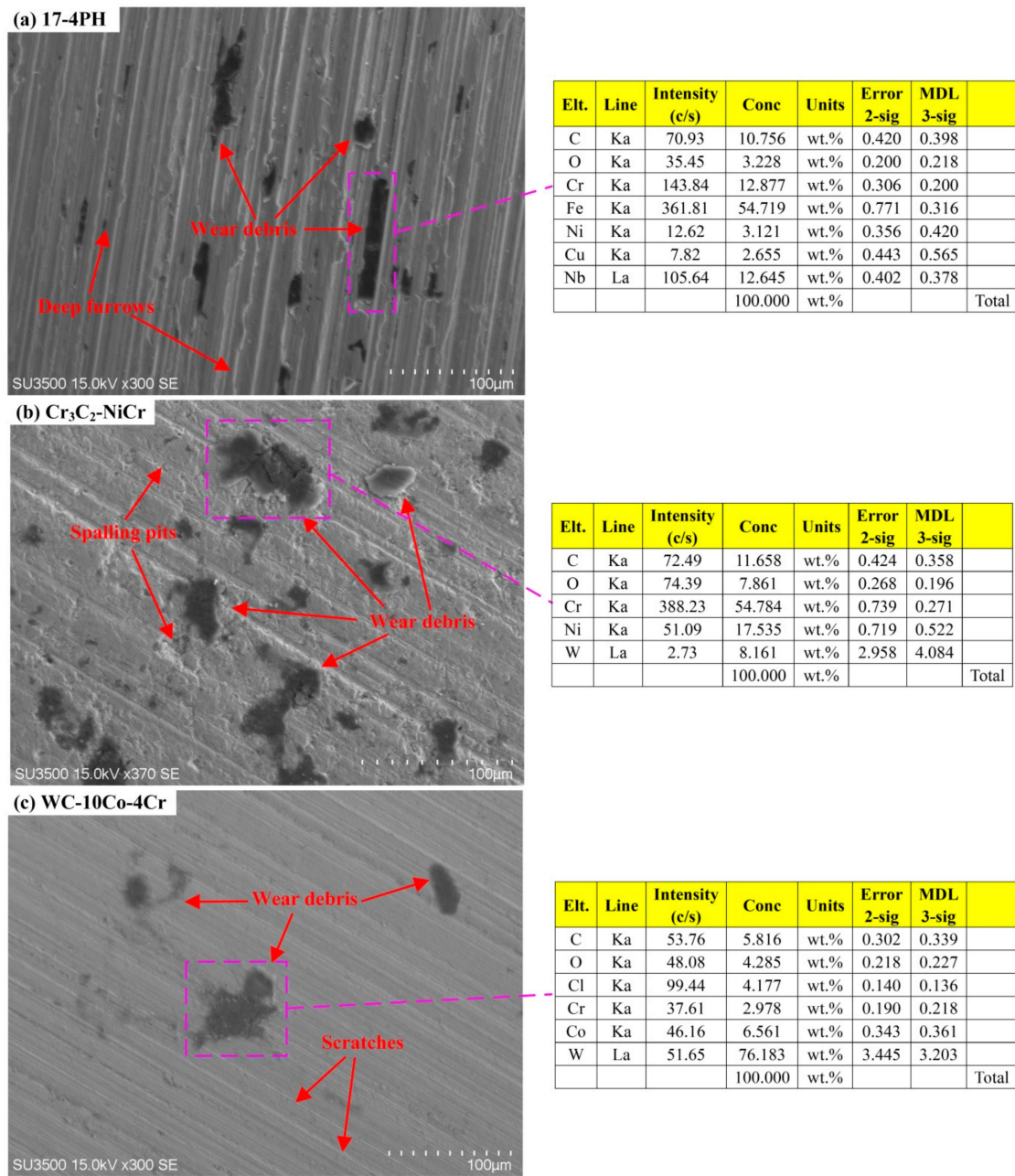


Figure 6. Cont.

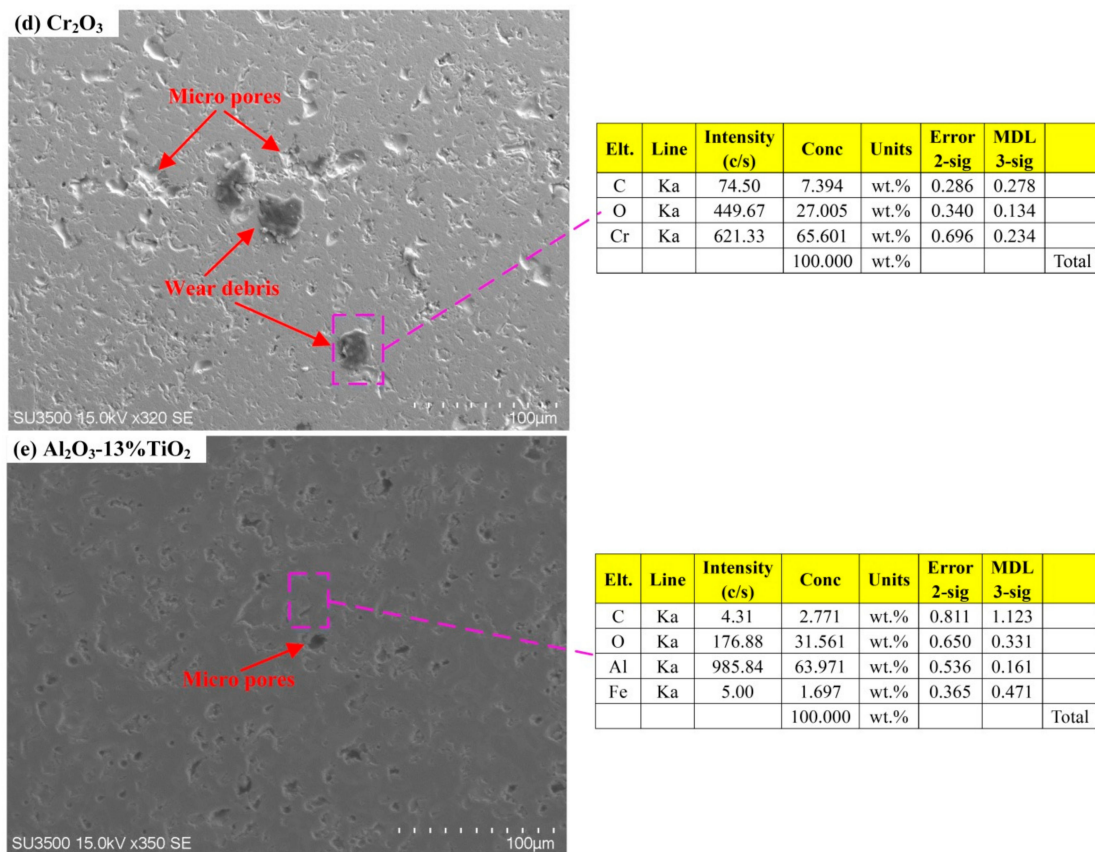


Figure 6. Worn surfaces morphology and the corresponding EDS results of different cermet coatings (100 N, 300 r/min): (a) 17-4PH; (b) Cr₃C₂-NiCr; (c) WC-10Co-4Cr; (d) Cr₂O₃ and (e) Al₂O₃-13%TiO₂.

3.3. Wear Track Analysis

The cross-sectional profiles and corresponding data of wear scar of the 17-4PH and several coatings under 100 N and 300 r/min are displayed in Figure 7 and Table 4, respectively. It is clearly shown in Figure 7a and Table 4 that the depth and width of the wear scar of 17-4PH were about 40 µm and 2.19 mm, respectively, which were higher than those of WC-10Co-4Cr, Cr₂O₃ and Al₂O₃-13%TiO₂ coatings. This indicates that the WC-10Co-4Cr, Cr₂O₃ and Al₂O₃-13%TiO₂ coated surfaces were less damaged than the uncoated surface of 17-4PH. However, the wear scar depth and width of the Cr₃C₂-NiCr coating were higher than other lower specimens. It is inferred that the Cr₃C₂-NiCr coating underwent severe wear at high rotational speed, which is in accord with the wear rates and worn surfaces morphology in Figures 4b and 6b, respectively. In addition, as illustrated in Figure 7e and Table 4, the maximum depth and width of the wear track of the Al₂O₃-13%TiO₂ coating were about 35 and 1.48 mm, which were the lowest values among these tribopairs. In addition, this result could indirectly explain why the friction coefficient of CF-PEEK/Al₂O₃-13%TiO₂ tribopair was relatively minimal under 100 N and 300 r/min (Figure 3).

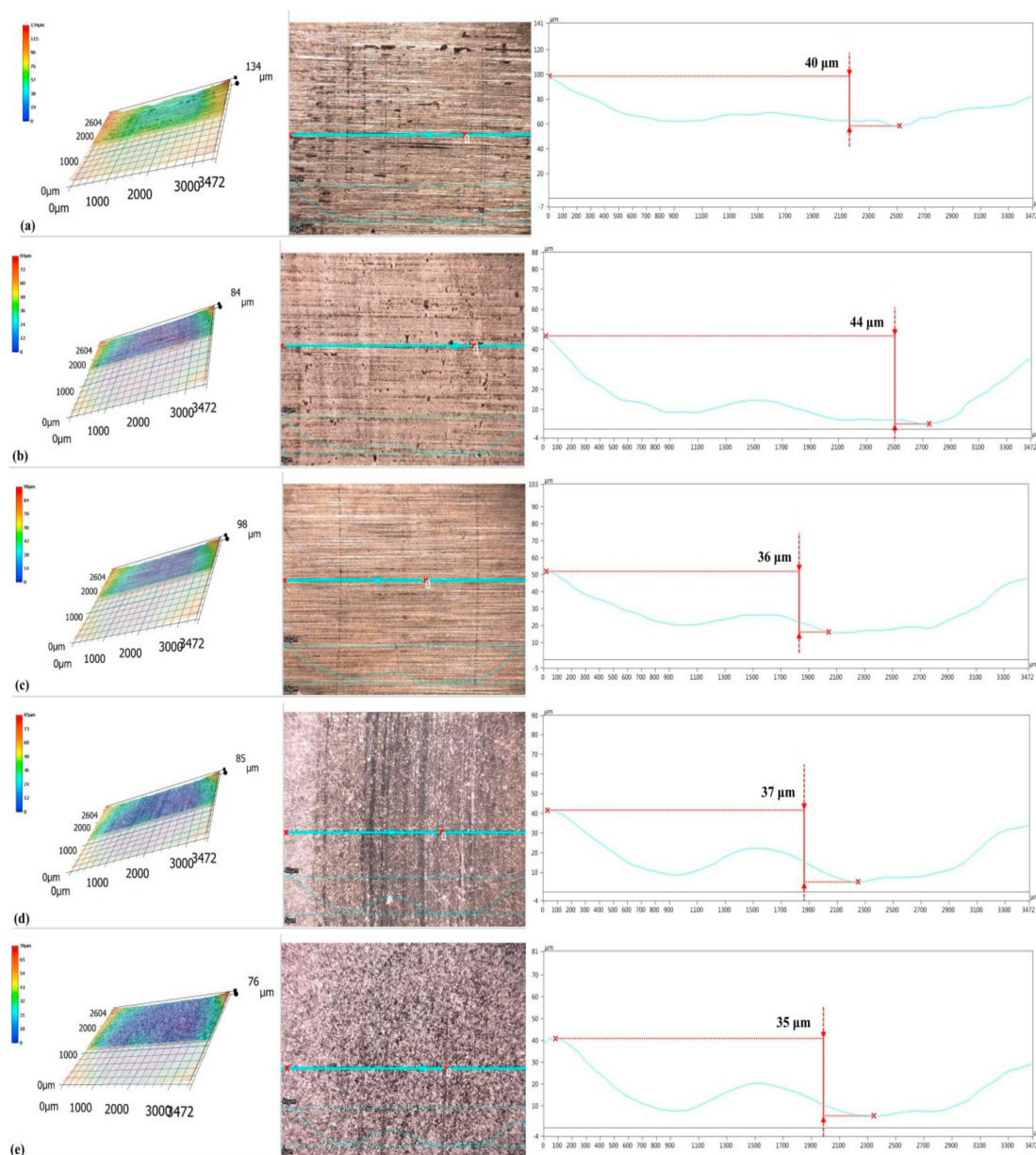


Figure 7. Worn surface scars of the lower specimens (100 N, 300 r/min): (a) 17-4PH; (b) $\text{Cr}_3\text{C}_2\text{-NiCr}$; (c) WC-10Co-4Cr; (d) Cr_2O_3 and (e) $\text{Al}_2\text{O}_3\text{-13\%TiO}_2$.

Table 4. Wear track results of the lower specimens (100 N, 300 r/min).

Specimen	Wear Scar Depth (μm)	Wear Scar Width (μm)
17-4PH	40	2194
$\text{Cr}_3\text{C}_2\text{-NiCr}$ Coating	44	3041
WC-10Co-4Cr Coating	36	2002
Cr_2O_3 Coating	37	2291
$\text{Al}_2\text{O}_3\text{-13\%TiO}_2$ Coating	35	1482

This is due to the fact that the $\text{Al}_2\text{O}_3\text{-13\%TiO}_2$ can react tribo-chemically with water to produce a reaction film in the sliding process. In addition, the reaction process can be described as follows: $\text{Al}_2\text{O}_3 + 3\text{H}_2\text{O} = 2\text{Al}(\text{OH})_3$ [15]. As the reaction film is easily sheared randomly, a low friction coefficient and wear rate of CF-PEEK/ $\text{Al}_2\text{O}_3\text{-13\%TiO}_2$ tribopair can be obtained in water. However, as the CF-PEEK slid against 17-4PH, $\text{Cr}_3\text{C}_2\text{-NiCr}$, WC-10Co-4Cr and Cr_2O_3 , these tribopairs could not react easily

with water [23]. Consequently, the tribological behaviors of CF-PEEK/17-4PH, CF-PEEK/Cr₃C₂-NiCr, CF-PEEK/WC-10Co-4Cr, CF-PEEK/Cr₂O₃ tribopairs were worse than that of CF-PEEK/Al₂O₃-13%TiO₂ tribopair. In addition, to improve the tribological behaviors of tribopairs in WHAPP and for further proving the important findings in this research, the material combination of CF-PEEK/Al₂O₃-13%TiO₂ will be applied to the key tribopairs in the pump prototype. Moreover, it will be one of the main research topics in the future to conduct long-term experimental research on WHAPP prototype, to study its tribological performance under actual size and working conditions, and to deal with the electrochemical corrosion of friction pairs for our seawater hydraulic components [24].

4. Conclusions

The tribological performance of CF-PEEK composite coupled with 17-4PH stainless steel and 17-4PH coated with Cr₃C₂-NiCr, WC-10Co-4Cr, Cr₂O₃ and Al₂O₃-13%TiO₂ in water was comparatively investigated. By varying the rotational speed from 100 to 300 r/min, it has been found that the higher speed is beneficial to improving the tribological behaviors for 17-4PH, WC-10Co-4Cr, Cr₂O₃ and Al₂O₃-13%TiO₂ coatings, while the increase of speed makes the tribological performance of Cr₃C₂-NiCr coating worse, and the Cr₃C₂-NiCr coating could be damaged under 100 N and 300 r/min lubricated with water. Proper increase of the surface hardness of 17-4PH by cermet coatings can improve the wear resistance of the tribopairs in water. However, the large hardness difference between the CF-PEEK and cermet coatings could accelerate the wear of the soft CF-PEEK. The CF-PEEK/Al₂O₃-13%TiO₂ material combination presents the best friction and wear performance among the tested five combinations under water lubrication conditions. The proposed CF-PEEK/Al₂O₃-13%TiO₂ tribopair has potential to replace the existing material combination of stainless steel and PEEK, and the working performance of the water hydraulic piston pump will be further improved.

Author Contributions: S.N. made the conception of the work and revised the manuscript critically for tribological analysis; F.L. performed the experiments and analyzed the data; H.J. carried out experimental design and wrote the manuscript; F.Y. wrote the literature review and other parts of the content.

Funding: The authors would like to thank the Beijing Natural Science Foundation (Grant Nos. 3182003 and 1184012), National Natural Science Foundation of China (Grant Nos. 51705008 and 11572012), Beijing Municipal Science and Technology Project (Grant Nos. KM201810005014 and KM201910005033), International Research Cooperation Seed Fund of Beijing University of Technology (Grant No. 2018B17) and CSIC Key Laboratory of Thermal Power Technology Open Foundation (Grant No. TPL2017AB010) for their funding for this research.

Acknowledgments: We are grateful to Xiaoyan Song and Haibin Wang for offering necessary assistance of the HVOF technique, and the editors and the anonymous reviewers for their insightful comments and suggestions.

Conflicts of Interest: The authors declare no conflict of interest.

References

1. Yang, H.Y.; Pan, M. Engineering research in fluid power: A review. *J. Zhejiang Univ.-Sci. A* **2015**, *16*, 427–442. [[CrossRef](#)]
2. Zhu, Y.; Chen, X.; Zou, J.; Yang, H. A study on the influence of surface topography on the low-speed tribological performance of port plates in axial piston pumps. *Wear* **2015**, *338–339*, 406–417. [[CrossRef](#)]
3. Zhang, J.H.; Chen, Y.; Xu, B.; Chao, Q.; Zhu, Y.; Huang, X.C. Effect of surface texture on wear reduction of the tilting cylinder and the valve plate for a high-speed electro-hydrostatic actuator pump. *Wear* **2018**, *414–415*, 68–78. [[CrossRef](#)]
4. Ye, S.G.; Zhang, J.H.; Xu, B.; Zhu, S.Q.; Xiang, J.W.; Tang, H.S. Theoretical investigation of the contributions of the excitation forces to the vibration of an axial piston pump. *Mech. Syst. Signal. Process.* **2019**, *129*, 201–217. [[CrossRef](#)]
5. Drablos, L.S. Testing of DanfossAPP1.0-2.2 with APP pumps as water hydraulic motors for energy recovery. *Desalination* **2005**, *183*, 41–54. [[CrossRef](#)]
6. Yin, F.L.; Nie, S.L.; Ji, H.; Huang, Y.Q. Non-probabilistic reliability analysis and design optimization for valve-port plate pair of seawater hydraulic pump for underwater apparatus. *Ocean Eng.* **2018**, *163*, 337–347. [[CrossRef](#)]

7. Lim, G.H.; Chua, P.S.K.; He, Y.B. Modern water hydraulics-the new energy-transmission technology in fluid power. *Appl. Energy* **2003**, *76*, 239–246. [[CrossRef](#)]
8. Majdič, F.; Pezdirnik, J.; Kalin, M. Experimental validation of the lifetime performance of a proportional 4/3 hydraulic valve operating in water. *Tribol. Int.* **2011**, *44*, 2013–2021. [[CrossRef](#)]
9. Mohanty, M.; Smith, R.W.; Bonte, M.D.; Celis, J.P.; Lugscheider, E. Sliding wear behavior of thermally sprayed 75/25 Cr₃C₂/NiCr wear resistant coatings. *Wear* **1996**, *198*, 251–266. [[CrossRef](#)]
10. Wei, J.; Xue, Q. The friction and wear properties of Cr₂O₃ coating with aqueous lubrication. *Wear* **1996**, *199*, 157–159. [[CrossRef](#)]
11. Zavareh, M.A.; Ahmed, A.D.M.S.; Bushroa, B.R.; Wan, J.B. The tribological and electrochemical behavior of HVOF-sprayed Cr₃C₂-NiCr ceramic coating on carbon steel. *Ceram. Int.* **2015**, *41*, 5387–5396. [[CrossRef](#)]
12. Huang, W.; Xu, Y.; Zheng, Y.; Wang, X.L. The tribological performance of Ti (C, N) -based cermet sliding against Si₃N₄ in water. *Wear* **2011**, *270*, 682–687. [[CrossRef](#)]
13. Wu, D.F.; Liu, Y.S.; Li, D.L.; Zhao, X.F.; Ren, X.J. The applicability of WC–10Co–4Cr/Si₃N₄ tribopair to the different natural waters. *Int. J. Refract. Met. Hard Mater.* **2016**, *54*, 19–26. [[CrossRef](#)]
14. Wu, D.F.; Liu, Y.S.; Zhao, X.F.; Li, D.L.; Ren, X.J. The tribological behaviors of different mass ratio Al₂O₃-TiO₂ coatings in water lubrication sliding against Si₃N₄. *Tribol. Trans.* **2016**, *59*, 352–362. [[CrossRef](#)]
15. Wang, C.T.; Ye, Y.W.; Guan, X.Y.; Hu, J.M.; Wang, X.; Li, J.L. An analysis of tribological performance on Cr/GLC film coupling with Si₃N₄, SiC, WC, Al₂O₃ and ZrO₂ in seawater. *Tribol. Int.* **2016**, *96*, 77–86. [[CrossRef](#)]
16. Strmcnik, E.; Majdič, F.; Kalin, M. Water-lubricated behaviour of AISI 440C stainless steel and a DLC coating for an orbital hydraulic motor application. *Tribol. Int.* **2019**, *131*, 128–136. [[CrossRef](#)]
17. Qiu, B.J.; Zhao, J.Y.; Man, J.X. Comparative study of materials for friction pairs in a new high water-based hydraulic motor with low speed and high pressure. *Ind. Lubr. Tribol.* **2019**, *71*, 164–172. [[CrossRef](#)]
18. Zhu, S.Y.J.; Ma, Q.; Tan, H.; Cheng, J.; Yu, Y.; Qiao, Z.H.; Yang, J. Tribological behavior of nickel aluminum-silver solid-lubricating alloy coupled with different tribo-pairs lubricated by seawater. *Tribol. Int.* **2019**, *131*, 158–166. [[CrossRef](#)]
19. Chen, B.B.; Wang, J.Z.; Yan, F.Y. Comparative investigation on the tribological behaviors of CF/PEEK composites under sea water lubrication. *Tribol. Int.* **2012**, *52*, 158–166. [[CrossRef](#)]
20. Wang, Z.Q.; Gao, D.R. Comparative investigation on the tribological behavior of reinforced plastic composite under natural seawater lubrication. *Mater. Des.* **2013**, *51*, 983–988. [[CrossRef](#)]
21. Dong, W.T.; Nie, S.L.; Zhang, A.Q. Tribological behavior of PEEK filled with CF/PTFE/Graphite sliding against stainless steel surface under water lubrication. *Proc. Inst. Mech. Eng. J-J. Eng.* **2013**, *227*, 1129–1137. [[CrossRef](#)]
22. Zhang, Z.H.; Nie, S.L.; Yuan, S.H.; Liao, W.J. Comparative evaluation of tribological characteristics of CF/PEEK and CF/PTFE/Graphite filled PEEK sliding against AISI630 steel for seawater hydraulic piston pumps/motor. *Tribol. Trans.* **2015**, *58*, 1096–1104. [[CrossRef](#)]
23. Hochstrasser, S.; Mueller, Y.; Latkoczy, C.; Virtanen, S.; Schmutz, P. Analytical characterization of the corrosion mechanisms of WC–Co by electrochemical methods and inductively coupled plasma mass spectroscopy. *Corros. Sci.* **2007**, *49*, 2002–2020. [[CrossRef](#)]
24. Zhang, J.; Su, X.L.; Shan, L.; Liu, Y.; Zhang, P.; Jia, Y. Preparation and tribocorrosion performance of CrCN coatings in artificial seawater on different substrates with different bias voltages. *Ceram. Int.* **2019**, *45*, 9901–9911. [[CrossRef](#)]

